Generalized Synchronization of Spatiotemporal Chaos in a Liquid Crystal Spatial Light Modulator

Elizabeth A. Rogers,[1,2,*] Rita Kalra,[2] Robert D. Schroll,[2] Atsushi Uchida,[2] Daniel P. Lathrop,[1,2,3] and Rajarshi Roy[1,2,3]

[1]*Department of Physics, University of Maryland, College Park, Maryland 20742, USA*

[2]*IREAP, University of Maryland, College Park, Maryland 20742, USA*

[3]*IPST, University of Maryland, College Park, Maryland 20742, USA*

(Received 25 February 2004; published 17 August 2004)

We demonstrate generalized synchronization in a spatiotemporal chaotic system, a liquid crystal spatial light modulator with optoelectronic feedback.

DOI: 10.1103/PhysRevLett.93.084101 PACS numbers: 05.45.Xt, 42.40.Eq, 42.65.Sf

Patterns in spatiotemporal systems are evident in nature and have been investigated extensively for many years [1]. Experiments and numerical models of pattern formation have revealed and explained different aspects of these intriguing phenomena. A most interesting dynamical aspect of pattern formation that is only beginning to be explored is the question of spatiotemporal synchronization, particularly for chaotic systems. In the past decade, a great variety of temporal synchronization phenomena have been reported for chaotic systems, including identical, phase, lag, and generalized synchronization [2]. However, it is only very recently that there have been efforts to demonstrate identical synchronization of spatiotemporal chaotic patterns [3].

Measurements of drive and response signals in extended spatiotemporal systems may have important applications in methods for noninvasive testing and monitoring of structures and materials, ranging from buildings to nanostructures such as biomolecules. They could also be used for computing in optical systems and encoded communications systems, including parallel communications. The dynamical synchronization of spatial patterns could have applications to spatiotemporal communication [4], which provides a practical motivation for the work presented here. The dynamics and patterns of the drive and response systems may differ greatly in character when generalized synchronization occurs and may provide an additional element of camouflage for message information.

While identical synchronization is more easily understood, detected, and quantified, generalized synchronization presents a much greater challenge to the experimentalist. Theoretically, generalized synchronization may be shown to exist between the drive and response systems through the predictability [5] or the existence of a functional relationship [6]. These approaches have been implemented in numerical models but are often difficult to implement in experimental measurements, due to the presence of noise and lack of precision. The auxiliary system method has been suggested for detecting generalized synchronization [7] when replicas or duplicates of the response system are available. In this method, the drive system is coupled to two or more response systems. If, after starting from different initial conditions, the response systems display identical synchronization after a period of transient dynamics dependent on system parameters, we can conclude that the response signal is generally synchronized to the drive [7]. In recent experiments, generalized synchronization has been observed in a one-dimensional laser system with optoelectronic feedback using the auxiliary method. This has been seen when systems with many degrees of freedom are coupled together by only a few variables or a lumped variable [8].

In this Letter, we demonstrate generalized synchronization experimentally in a spatiotemporally chaotic two-dimensional system. An optoelectronic feedback loop using a liquid crystal spatial light modulator (SLM) is a flexible method for generating spatiotemporal patterns and has been used in this manner over the last 20 years [9–11]. These patterns range from hexagonal close packed dot structures to spatiotemporal chaos. Numerical models of liquid crystal SLM behavior show a variety of regular and irregular patterns that correspond well to experiments [10]. We use the auxiliary system method to show that generalized synchronization occurs between a recorded and replayed sequence of drive and response patterns.

In our experiments, the reference light beam from a linearly polarized 633 nm helium neon laser is incident on a Hamamatsu computer controlled, electrically addressed liquid crystal SLM, as shown in the experimental setup of Fig. 1. After reflecting off of the phase grating, the beam propagates for approximately 2.5 m before it is incident on a Pulnix TM-72EX charge coupled device (CCD) camera. The SLM uses the videographics array output to make a gray-scale pattern on an internal liquid crystal display (LCD). Though the liquid crystal is not pixilated, the LCD consists of an array of 640×480 pixels, 480×480 of which are active and of which the central 244×360 are used in this experiment. The image from the camera is then displayed on a computer monitor

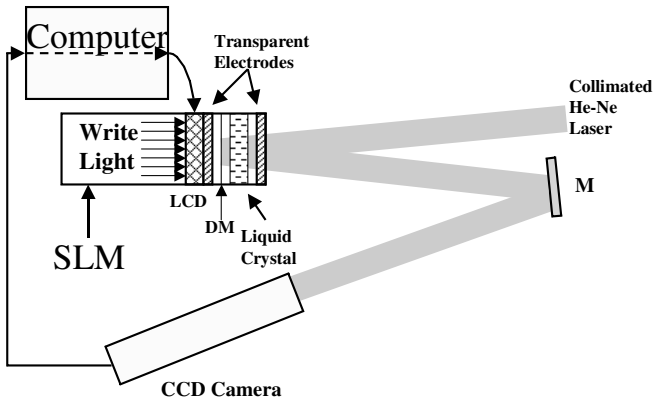

FIG. 1. Experimental setup for generalized synchronization of spatiotemporal chaos: SLM, spatial light modulator; M, mirror; LCD, liquid crystal display; DM, dielectric mirror.

and also transferred to the SLM. The camera detects 114×180 pixels from the center of the diffracted beam and the inverted image is displayed on the array of 244×360 pixels in the center of the LCD. Therefore, we use an inverted stretched image of the central portion of our beam as the feedback signal over the utilized area of the SLM. An internal laser provides a write light beam that propagates through the LCD onto the back of an amorphous silicon photoconductive layer coated on transparent glass plates, which place voltages across the liquid crystal. This creates the phase grating, as shown in Fig. 1. Thus the intensity pattern, created by the initial phase grating and displayed on the monitor, transforms the liquid crystal into a new phase grating which, in turn, modulates the laser beam and the process repeats, again as shown in Fig. 1. The time scales for the liquid crystal are approximately 30 ms for turn on (this depends on the bias voltage) and approximately 40 ms for relaxation into the off state. The LCD refresh rate is 30 Hz. The pattern evolution time scale depends on the bias voltage and the refresh rate of the LCD. These time scales are all roughly comparable in the regime of operation of the experiment.

The closed-loop (the configuration that includes the broken arrow in Fig. 1) intensity patterns are recorded for approximately 17 s on a Silicon Graphics Inc. O_2 Media Recorder in Apple Quicktime format at a rate of 30 frames/s. The resulting sequence of patterns (a movie) that are generated from the closed loop are spatiotemporally chaotic and serve as the drive signals in the auxiliary system method. In previous experimental and numerical studies of liquid crystal pattern formation, the route to chaos via destabilization of regular patterns is governed by the intensity of the write light [9–11]. In our system, the write light intensity is fixed, and when the SLM is in a feedback loop, we see chaos immediately, if the bias voltage exceeds a threshold value of 1.5 V.

In our experiments, the parameter we vary is the bias voltage. Drive movies were recorded at bias voltages between 1.50 and 5.00 V at 0.25 V increments. Bias voltage plays an important role in determining the properties of the optical turbulence that we observe in the closed-loop system. Figure 2(a) shows a typical picture of the images that appear when the SLM is run in a closed loop. The average grain size depends on the applied bias voltage, the smallest grain size appearing at the middle bias voltage levels and the largest appearing at bias voltages closer to the minimum and maximum values. The grain sizes were determined using a two-dimensional autocorrelation function after subtracting the mean value of each image. The full width at half maximum (FWHM) was then calculated and an average grain size was extracted. The autocorrelation function and average grain size as a function of bias voltages for a variety of drive signals can be seen in Fig. 2(b) and 2(c), respectively. The spatial Fourier spectra were also calculated, and they correspond well to the autocorrelation results.

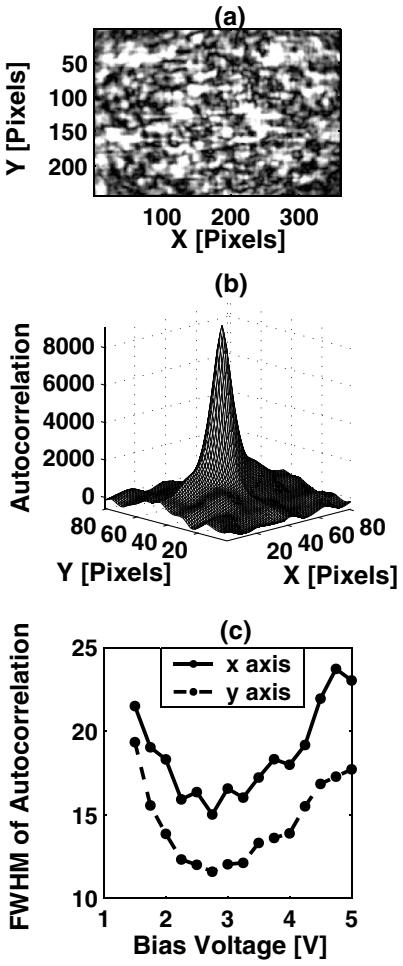

FIG. 2. (a) is a typical far field chaotic pattern generated by the SLM in the closed-loop feedback system. (b) is a 3D plot of the autocorrelation from which we take 2D slices at the peak in the x and the y direction. We calculate the FWHM of the slices and, from this, the grain size. (c) is a plot of the average grain size in the x and y direction versus the bias voltage.

To test for generalized synchronization, an open-loop configuration is created by breaking the connection shown by the dashed line in Fig. 1, and a second computer is connected to the SLM. The drive movie stored on the original computer is "played" into the SLM by the second computer and the SLM response to the drive movie is recorded on the original computer. Several response signals to the same drive signal are recorded in order to implement the auxiliary system test for generalized synchronization. Additionally, the initial conditions of each response movie are made to differ by placing a different initial frame on the drive movie each time it was played. The intensity patterns of the response movies are then compared with each other, frame-by-frame and pixel-by-pixel, in order to see if the response system is generally synchronized to the drive system. The experiment was repeated for different values of the SLM bias voltage. Since all of the movies are recorded on the same setup, all images undergo the same transformations.

Figure 3 shows typical snapshots of the drive and two response movies at the same frame number. It is evident that the drive and response images look very dissimilar but that response 1 and response 2 are nearly identical, which is consistent with generalized synchronization. The quality of the synchronization is quantified by the synchronization error. This is the difference of the gray-scale values at each two-dimensional spatial location (pixel) between the images of the two response movies, $\langle e(x, y, t)\rangle = 10 \times \log_{10}\langle|[I_A(x, y, t) - I_B(x, y, t)]|\rangle$, where the angle brackets denote space and time averaging. $I_A(x, y, t)$ and $I_B(x, y, t)$ are the normalized intensities of the two response images at the position of (x, y) at the time of t in the two response movies. For calibration, the synchronization error was computed for the response of the SLM to the same static image at two different times and was found to be approximately -30 dB. Therefore, a synchronization error of less than -25 dB was defined as the threshold for generalized synchronization. The results of this analysis are presented in Fig. 4(a), where the transient period before synchronization is a result of the mismatched initial conditions, and time is represented by the frame number of the movie. The movies analyzed were responses to a drive movie taken at a bias voltage of 1.5 V. Initially, the responses are unsynchronized, but

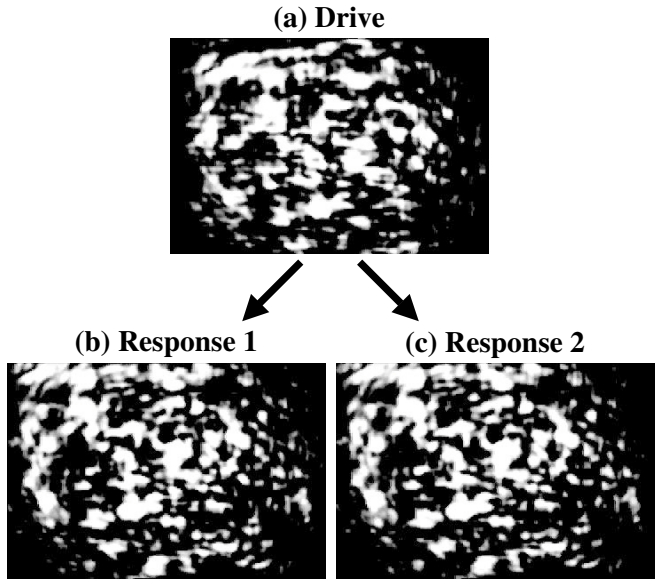

FIG. 3. Typical far field chaotic patterns generated by the SLM in the closed-loop drive system (a) and the open-loop response system (b),(c), at 1.5 V bias voltage. The chaotic patterns for the two responses are well synchronized both spatially and temporally.

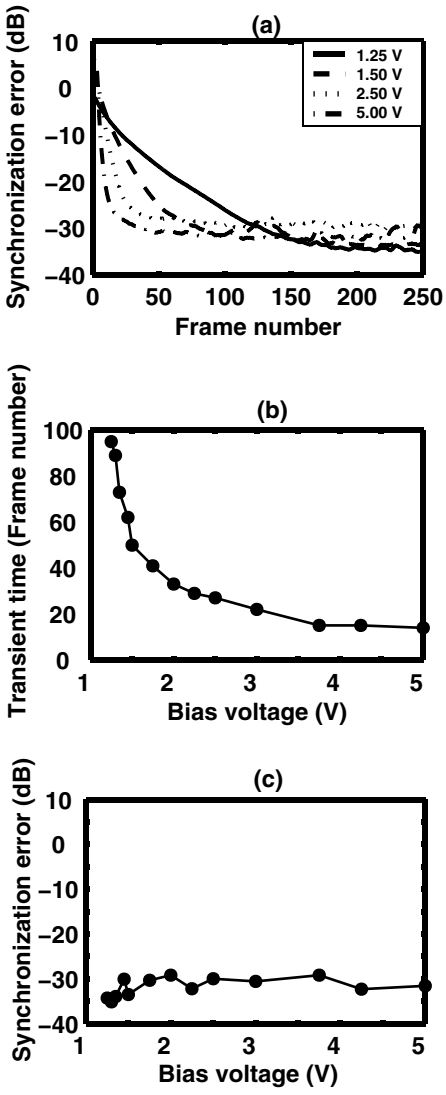

FIG. 4. Characteristics of generalized synchronization. (a) Transients of generalized synchronization error at different bias voltages of the SLM. (b) Transient time (frame number) of generalized synchronization as a function of bias voltage. The threshold for synchronization is set at -25 dB. (c) Generalized synchronization error at different bias voltages after the transient period.

the synchronization level increases (error decreases) with time and converges to an error of −30 dB.

The system shows transient behavior on time scales that depend on the bias voltage. The first frame of the drive movie was changed each time the drive movies were played to the response system, but the changes in initial conditions were identical for each bias voltage. However, the system response to these changes varied depending on the response bias voltage, as did the time the responses took to synchronize. Figures 4(b) and 4(c) show how the synchronization error depends on the bias voltage of the response system. Transient time monotonically decreases as the bias voltage increases, which indicates that responses taken at high bias voltages synchronize to the drive signal more quickly than those at low bias voltages. Generalized synchronization error after the transient process was also investigated as a function of bias voltage. Figure 4(c) demonstrates that the synchronization error is approximately constant for all values of the response bias voltage once synchronization occurs. The system, therefore, reacted to the change in initial conditions differently for each bias voltage. When a static image is placed on the SLM, tuning the bias voltage affects only the spatial resolution of the image; it does not change the image itself. In the dynamic case studied here, tuning the bias voltage results in changes in the images formed in response to the same drive images. The different transient responses of the SLM at different bias voltages are evidence that the SLM is not just acting as a passive filtering device, but that the generalized synchronization is a product of dynamics internal to the device.

We can conclude that the response system displays generalized synchronization to the drive, independent of initial conditions. Since the dynamics of the response system are repeatable and reproducible, generalized synchronization is stably achieved in this system. We do not observe identical synchronization in our experiments. The reason for observing only generalized synchronization is a loss of information in the recorded movies at each iteration of the feedback loop. Feeding back only the center portion of the diffracted beam leads to a significant loss of information and resolution of the spatial pattern. All of these issues result in a recorded movie that has lost various spatiotemporal degrees of freedom, corresponding to hidden variables in the system. This is analogous to loss of modal information corresponding to hidden degrees of freedom in the experiment presented in Ref. [8].

In conclusion, we have observed generalized synchronization of spatiotemporal chaos in an optoelectronic feedback system with a liquid crystal SLM. The transient characteristics of generalized synchronization depend on the bias voltage of SLM, whereas the generalized synchronization error is almost constant at various bias voltages after transient.

We acknowledge support from the Physics Division of the U.S. Office of Naval Research. E. A. R. acknowledges support from the National Science Foundation. R. K. acknowledges support from the TREND NSF REU program at IREAP, University of Maryland. A. U. thanks the Japan Society for the Promotion of Science for support.

*Electronic address: rogerse@glue.umd.edu.

[1] M. I. Rabinovich, A. B. Ezersky, and P. D. Weidman, *The Dynamics of Patterns* (World Scientific, Singapore, 2000).

[2] L. M. Pecora and T. L. Carroll, Phys. Rev. Lett. **64**, 821 (1990); A. Pikovsky, M. Rosenblum, and J. Kurths, *Synchronization* (Cambridge University Press, Cambridge, 2001); S. Boccaletti, J. Kurths, G. Osipov, D. L. Valladares, and C. S. Zhou, Phys. Rep. **366**, 1 (2002).

[3] J. Bragard, S. Boccaletti, and F. T. Arecchi, Int. J. Bifurcation Chaos Appl. Sci. Eng. **11**, 2715 (2001); R. Neubecker and B. Gütlich, nlin.PS/0304052; R. Neubecker and B. Gutlich, Phys. Rev. Lett. **92**, 154101 (2004).

[4] J. García-Ojalvo and R. Roy, Phys. Rev. Lett. **86**, 5204 (2001).

[5] N. F. Rulkov, M. M. Sushchik, L. S. Tsimring, and H. D. I. Abarbanel, Phys. Rev. E **51**, 980 (1995); S. J. Schiff, P. So, T. Chang, R. E. Burke, and T. Sauer, Phys. Rev. E **54**, 6708 (1996); K. Yoshimura, Phys. Rev. E **60**, 1648 (1999); M. Wiesenfeldt, U. Parlitz, and W. Lauterborn, Int. J. Bifurcation Chaos Appl. Sci. Eng. **11**, 2217 (2001).

[6] R. Brown, Phys. Rev. Lett. **81**, 4835 (1998); J. Arnhold, P. Grassberger, K. Lehnertz, and C. E. Elger, Physica (Amsterdam) **134D**, 419 (1999); C. L. Goodridge, L. M. Pecora, T. L. Carroll, and F. J. Rachford, Phys. Rev. E **64**, 026221 (2001); V. Afraimovich, A. Cordonet, and N. F. Rulkov, Phys. Rev. E **66**, 016208 (2002); B. R. Hunt, E. Ott, and J. A. Yorke, Phys. Rev. E **55**, 4029 (1997).

[7] H. D. I. Abarbanel, N. F. Rulkov, and M. M. Sushchik, Phys. Rev. E **53**, 4528 (1996); L. Kocarev and U. Parlitz, Phys. Rev. Lett. **76**, 1816 (1996); K. Pyragas, Phys. Rev. E **54**, R4508 (1996); D. Y. Tang, R. Dykstra, M. W. Hamilton, and N. R. Heckenberg, Phys. Rev. E **57**, 5247 (1998).

[8] A. Uchida, R. McAllister, R. Meucci, and Rajarshi Roy, Phys. Rev. Lett. **91**, 174101 (2003).

[9] G. D'Alessandro and W. K. Firth, Phys. Rev. A **46**, 537 (1992); R. Neubecker, B. Thuering, M. Kreuzer, and T. Tschudi, Chaos Solitons Fractals **10**, 681 (1999).

[10] R. Neubecker, G. L. Oppo, B. Thuering, and T. Tschudi, Phys. Rev. A **52**, 791 (1995); B. Thuring *et al.*, Asian J. Phys. **7**, 453 (1998).

[11] M. A. Vorontsov, J. C. Ricklin, and G. W. Carhart, Opt. Eng. (N.Y.) **34**, 3229 (1995); P. L. Ramazza, S. Ducci, S. Boccaletti, and F. T. Arecchi, J. Opt. B **2**, 399 (2000).